

# The cosmological evolution of colour gradients in spheroids

A. C. S. Friaça<sup>1</sup> and R. J. Terlevich<sup>2,3</sup>

<sup>1</sup>*Instituto Astronômico e Geofísico, USP, Av. Miguel Stefano 4200, 04301-904 São Paulo, SP, Brazil*

<sup>2</sup>*Institute of Astronomy, Madingley Road, Cambridge CB3 0EZ, UK*

<sup>3</sup>*Visiting Professor at Instituto Nacional de Astrofísica, Óptica y Electrónica. Av. Luis Enrique Erro 1, Tonanzintla, Puebla, Mexico*

16 November 2018

## ABSTRACT

The analysis of the four-colour maps of galaxies in the Hubble Deep Field has revealed in the sample of  $0.4 < z < 1$  early-type field galaxies the existence of ellipticals with a predominantly old coeval stellar population. However, there is another, unexpected, category of HDF early-type galaxies, in which the galaxy core is significantly bluer than the outer regions. We demonstrate that these colour gradients are predicted by the multi-zone chemodynamical model for the evolution of elliptical galaxies.

We suggest that the colour gradient could be used as a chronometer for the evolution of elliptical galaxies: galaxies younger than a few Gyr exhibit cores bluer than the surrounding galaxy, due to ongoing star formation while more evolved galaxies have redder cores, due to metallicity gradients increasing toward the centre.

**Key words:** cosmology: observations – galaxies: elliptical – galaxies: evolution – galaxies: formation – galaxies: ISM – galaxies: starburst

## 1 INTRODUCTION

A surprising result of the analysis of the four-colour ( $U_{300}B_{450}V_{606}I_{814}$ ) maps of the Hubble Deep Field (Abraham et al. 1999, hereafter A99; Menanteau, Abraham & Ellis 2000) is the existence of early-type field galaxies, with positive colour gradients in the centre (galaxy nucleus bluer than the outer surrounding region) evidencing recent nuclear star formation in early-type galaxies with  $0.4 < z < 1$ .

Although these bluer core spheroids (BCSs) could be explained within the scenario of structure formation via hierarchical merging, in which the recent nuclear star formation would be the result of mergers leading to the formation of an elliptical galaxy, the high degree of symmetry in the images requires, additionally, that, after the merger, the systems had had time to relax to a spheroidal geometry.

On the other hand, the appearance of these systems is exactly that predicted by the chemodynamical model for evolution of elliptical galaxies (Friaça & Terlevich 1994; Friaça & Terlevich 1998, hereafter FT98). The chemodynamical model is a single collapse model, differing, however, from the monolithic collapse model, in that it is a multi-zone model, in which there is no coordination in the star formation in the several zones of the model. This allows that, locally, the time scales for star formation could be of the order of 0.1 Gyr in the central regions of the galaxy, leading to a super-solar [Mg/Fe] ratio as observed in luminous ellipticals, while it takes  $\sim 1$  Gyr for the main body of the elliptical galaxy to be formed. An important ingredient of the chemodynamical model is the persistence of a central

cooling flow for 2–3 Gyr, feeding star formation in the core, which would account for the core being bluer than the rest of the galaxy, as in the BCSs found in the HDF.

Within the frame of the chemodynamical model, the BCSs at intermediate redshifts would be one of the manifestations of the general evolution of spheroids. At higher redshifts, the chemodynamical model for the evolution of spheroids predicts a link of the BCSs with Lyman break galaxies (Steidel 1995, 1996) and the scarcity of passively evolving elliptical galaxies (Zepf et al. 1997, Barger et al. 1999). At  $z \sim 3$ , the first  $\sim 1$  Gyr of our model galaxies shows striking similarities to the Lyman break galaxies (LBGs): intense star formation, compact morphology, the presence of outflows, and significant metal content. Our investigation of the nature of the LBGs using the chemodynamical model for spheroids (Friaça & Terlevich 1999, hereafter FT99) supports a scenario in which LBGs are the progenitors of the present-day (age of 13 Gyr) moderately bright ( $0.05L^* - 1.4L^*$ ) spheroids. Over the  $z > 1$  range in general, the continuing (for  $\sim 2 - 3$  Gyr) star formation in the centre of ellipticals predicted by the chemodynamical model could explain the relative absence of very red galaxies in deep optical and near-infrared surveys, as expected from a population of passively evolving elliptical galaxies (Jimenez et al. 1999). The BCSs would indicate the persistence of the same continuing central star formation at redshift  $< 1$ . It should be noted, however, that most of the mass of the stellar population is formed during the first Gyr; typically half of the present stellar mass of the galaxy is formed in

$\sim 0.5$  Gyr, and  $\sim 5\% - 30\%$  during the extended lower level central star formation phase.

In this paper, we follow in detail the evolution of colour gradients in spheroids within the scenario of the chemodynamical model and investigate the relation of the continuing central star formation activity to the BCS population. Section 2 gives a description of the chemodynamical model. Section 3 presents the predicted evolution of colour gradients in spheroids. We show that, for a wide range of masses, there are 3 phases: 1) an earlier phase, with relatively flat colour gradients; 2) the bluer core phase; and 3) the redder core phase. Section 3 also discuss the possibility of using the transition from the bluer core phase to the redder core phase as an evolutionary clock in cosmological studies. Finally, in section 4, we identify the BCS seen at  $0.4 < z < 0.7$  as sub- $L^*$  spheroids formed at  $z > 1$  with continuing central star formation or recurrent bursts of central star formation. Section 4 summarises our conclusions.

We adopt in this paper  $H_0 = 70 \text{ km s}^{-1} \text{ Mpc}^{-1}$ , in accordance with the value obtained by HST Key Project on the Extragalactic Distance Scale,  $H_0 = 71 \pm 6 \text{ km s}^{-1} \text{ Mpc}^{-1}$ , or, including a possible metallicity dependence of the Cepheid period-luminosity relation,  $H_0 = 68 \pm 6 \text{ km s}^{-1} \text{ Mpc}^{-1}$  (Mould et al. 2000). We also adopt a flat  $\Omega_m + \Omega_\Lambda = 1$  cosmology.

## 2 THE CHEMODYNAMICAL MODEL

In this work, the evolution of spheroids is modelled with the aid of the chemodynamical model of FT98. The chemodynamical model combines multi-zone chemical evolution with 1-D hydrodynamics to follow in detail the evolution and radial behaviour of gas and stars during the formation of a spheroid. Within each spherical zone, in which the model galaxy has been divided for the 1-D hydrodynamical calculations, the evolution of the abundances of six chemical species (He, C, N, O, Mg, Fe) is calculated by solving the basic equations of chemical evolution. The star formation and the subsequent stellar feedback regulate episodes of wind, outflow, and cooling flow. The knowledge of the radial gas flows in the galaxy allows us to trace metallicity gradients, and, in particular, the formation of a high-metallicity core in ellipticals.

FT98 built a sequence of chemodynamical models reproducing the main properties of luminous elliptical galaxies. The calculations begin with a gaseous protogalaxy with initial baryonic mass  $M_G$ . FT98 investigates models with  $M_G$  between  $10^{11}$  and  $5 \times 10^{12} M_\odot$ . In order to study LBGs, FT99 have subsequently extended the mass grid of the models of FT98 downwards to  $5 \times 10^9 M_\odot$ . Intense star formation during the early stages of the galaxy builds up the stellar body of the galaxy, and during the evolution of the galaxy, gas and stars exchange mass through star formation and stellar gas return. Owing to inflow and galactic wind episodes occurring during the galaxy evolution, its present stellar mass is  $\sim 15 - 70\%$  higher than  $M_G$ . Gas and stars are embedded in a dark halo of core radius  $r_h$  and mass  $M_h$  (we set  $M_h = 3M_G$ ). The models are characterised by  $M_G$ ,  $r_h$ , and a star formation prescription. The SFR is given by a Schmidt law  $\nu_{SF} \propto \rho^{x_{SF}}$  ( $\rho$  is the gas density and  $\nu_{SF} = SFR/\rho$  is the specific SFR). Here we consider the

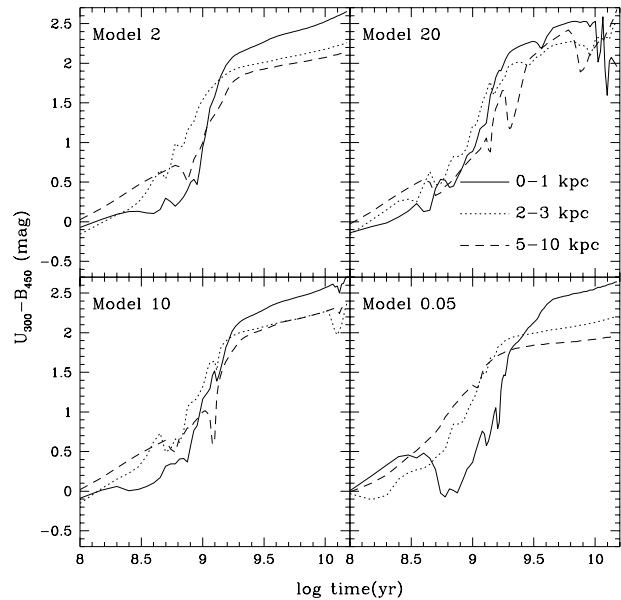


**Figure 1.** Evolution of the colour  $U_{300} - B_{450}$  (rest-frame) through several annular apertures for the models with  $M_G = 2 \times 10^{11} M_\odot$  (labeled Model 2), with  $M_G = 2 \times 10^{12} M_\odot$  (Model 20), with  $M_G = 10^{12} M_\odot$  (Model 10), and with  $M_G = 5 \times 10^9 M_\odot$  (Model 0.05).

standard star formation prescription of FT98, in which the normalization of  $\nu$  is  $\nu_0 = 10 \text{ Gyr}^{-1}$  (in order to reproduce the super-solar  $[\text{Mg}/\text{Fe}]$  ratio of giant ellipticals) and  $x_{SF} = 1/2$  (with the exception of one model, for which  $x_{SF} = 1/3$ ). The stars form in a Salpeter IMF from 0.1 to  $100 M_\odot$ . A more detailed account of the models can be found in FT98.

## 3 EVOLUTION OF COLOURS GRADIENTS

We have used the spectrophotometric models of Bruzual & Charlot (1998) to compute the SED for each galaxy zone. This is done in a self-consistent way using the metallicity given for each zone and each time by the chemodynamical model and for a consistent IMF. Then, the SED is integrated over several apertures, redshifted, reddened by the Lyman  $\alpha$  forest opacity (Madau 1995), and convoluted with the filter transmission curves. Unless otherwise stated, AB magnitudes are used throughout this paper.

It is helpful for the understanding the evolution of the colour gradients to consider first the evolution of the colours in the rest-frame of the galaxy. Figure 1 shows the evolution of the  $U_{300} - B_{450}$  colour, more sensitive to on-going star formation, as seen through several annular apertures, for several models, with  $M_G$  ranging from  $5 \times 10^9$  to  $M_G = 2 \times 10^{12} M_\odot$ . The evolution of model with  $M_G = 2 \times 10^{11}$  (the fiducial model of FT98, or model 2 —following FT98 we label the models according  $M_G$  in units of  $10^{11} M_\odot$ ) is typical of models covering a wide range of masses (from less than  $10^{10}$  up to  $10^{12} M_\odot$ ). Its evolution exhibits 3 distinct epochs regarding the colour gradients: 1) An early phase, during which the galaxy as a whole is blue, due to wide

spread intense star formation. The region with the highest SFR's extends out to  $r \sim 3$  kpc with little radial gradient of specific SFR, which results in a colour gradient flat in this region. The very central region can be even redder than its immediate surroundings during this phase, due to the very fast chemical enrichment for  $r < 1$  kpc (where, the metallicity, at 0.1 Gyr, of the stellar population is  $0.6 Z_\odot$ )

2) After  $3 \times 10^8$  yr, the SFR decreases from outside in, but it persists for more than 1 Gyr in the core ( $r < 1$  kpc), which is significantly bluer than the rest of the galaxy: that is the *bluer core* phase, during which the galaxy would be seen as a BCS; 3) The last phase ( $t > 1$  Gyr) is the *redder core* phase, during which the level of star formation is low in the core, which is redder than the outer parts of the galaxy, due to its high metallicity. The dips in the evolution of  $U_{300} - B_{450}$  indicates bursts of star formation. Note that the transition from bluer core phase to the redder core phase is rapid, which suggest the use of this transition as a time-marker. The transition occurs later if we consider the surrounding  $2 < r < 3$  kpc region, because in the outermost radii ( $5 < r < 10$  kpc), the lower metallicities imply bluer colours.

The evolution of the model with  $M_G = 2 \times 10^{12} M_\odot$  (model 20 of FT98) illustrates another sequence of phases that occurs only for very massive systems ( $M_G \gtrsim 10^{12} M_\odot$ ). In this mass range, the galactic wind occurs late, and the inner cooling flow stops for a short time after which it reappears and eventually becomes a massive, global cooling flow extending over 100 kpc. The bluer core is clearly present only in the early stages of the evolution (till  $\sim 0.3$  Gyr). After this time, due to the complex inner cooling flow behaviour, which extends over the whole  $r < 10$  kpc, several uncoordinated star formation episodes rend the colour gradients ill-defined. For  $t \gtrsim 1.5$  Gyr, the core is redder than its surroundings, although the transition of a bluer core to a redder core is not smooth, and the evolution of the colour of the core is subject to some blueing at  $\sim 3$  Gyr due to a weak, late, central star formation episode. Finally, in late times  $t \lesssim 10$  Gyr, the establishment of a massive, global cooling flow recovers a bluer core.

Note that, although the model with  $M_G = 10^{12} M_\odot$  is also massive enough to develop a cooling flow in  $t > 10$  Gyr, (visible as a dip in the  $U_{300} - B_{450}$  profiles after this time), during its first 10 Gyr it exhibits the three-phase evolution of the colour gradients, with the characteristic clear separation between the bluer core and the redder core stage at  $\sim 1$  Gyr.

### 3.1 A typical $\sim L^*$ galaxy

The fiducial model of FT98 ( $M_G = 2 \times 10^{11} M_\odot$  and  $r_h = 3.5$  kpc) has a present-day stellar mass,  $2.4 \times 10^{11} M_\odot$ , corresponding to  $L_B = 0.7 L^*$ , being typical for a present-day moderately luminous elliptical galaxy. Figure 2 shows the evolution of the colour gradient for this model. The quantity  $\Delta C$  is defined as the colour at an annulus  $5 < r < 10$  kpc minus the colour in the central kpc ( $r < 1$  kpc). Positive values of  $\Delta C$  therefore correspond to positive central colour gradients, and indicate a core bluer than the surrounding galaxy. The  $5 < r < 10$  kpc dimension chosen for the annulus representing the non-nuclear part of the galaxy falls inside a typical effective radius of a luminous elliptical ( $\sim 10$  kpc for a  $L^*$  elliptical). This region is easily resolvable by large ground-based telescopes, since 1 arcsec corre-

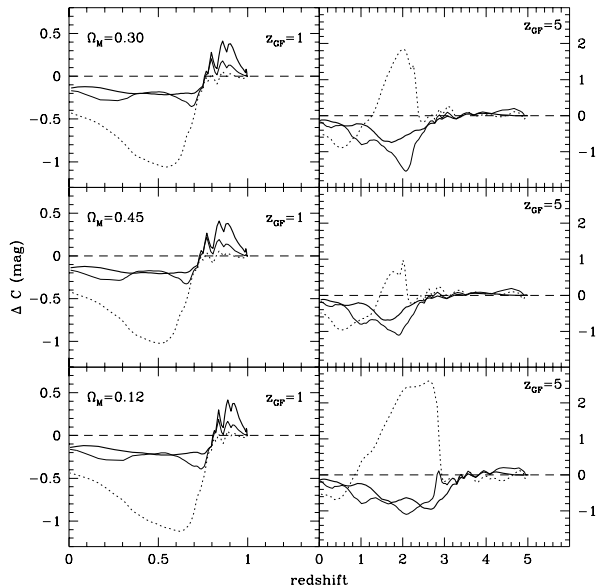


**Figure 2.** The evolution of the colour gradients  $\Delta C$  of the colours:  $V_{606} - I_{814}$  (heavy solid lines),  $B_{450} - V_{606}$  (light solid lines), and  $U_{300} - B_{450}$  (dotted lines), for the model with  $2 \times 10^{11} M_\odot$  and for several cosmologies and two epochs ( $z_{GF}$ ) of galaxy formation.

sponds to 8.0 (9.1, 7.4) kpc for  $H_0 = 70 \text{ km s}^{-1} \text{ Mpc}^{-1}$  and  $\Omega_m = 0.3$  ( $= 0.12, = 0.45$ ) (assuming a flat cosmology  $\Omega_m + \Omega_\Lambda = 1$ ). At the same time, the  $r < 10$  kpc region avoids the  $\propto (1+z)^{-4}$  Tolman dimming of the surface brightness which makes it difficult to detect the outermost regions of the galaxy, if it is at high redshifts. As we can see from Figure 2, the changes in the central colour gradient are more dramatic for an epoch of galaxy formation  $z_{GF} = 5$ , but they are very noticeable for  $z_{GF} = 1$ . If the galaxy is formed at a recent epoch ( $z_{GF} = 1$ ), the bluer core is more noticeable in the  $V_{606} - I_{814}$  colour, while for higher redshifts of galaxy formation, the  $U_{300} - B_{450}$  colour would trace better the continuing star formation in the galaxy centre. For instance, for  $z_{GF} = 5$ , the galaxy would have an bluer core for  $z < 3$  (when it is in the phase of central continuing star formation) only in the  $U_{300} - B_{450}$  colour (with a maximum around  $z = 2$  for  $z_{GF} = 5$ ), while for the  $B_{450} - V_{606}$  and  $V_{606} - I_{814}$  colours, the core is *redder* than the surrounding galaxy.

The bluer core phase may be characterised by  $z_{rev}$ , the redshift at which there is the reversal from blue core (due to central star formation) to red core (due to metallicity gradient). The values of  $z_{rev}$  are exhibited in Table 1 for the models, colours and cosmologies used in this paper.

The colour  $V_{606} - I_{814}$  (in which we can follow more closely the evolution of the colour gradient) has  $z_{rev} = 0.764$  for a  $\Omega_m = 0.3$ ,  $\Omega_\Lambda = 0.7$  cosmology and a recent galaxy formation epoch ( $z_{GF} = 1$ ). The maximum of  $V_{606} - I_{814}$  is  $\Delta C = 0.414$  at  $z = 0.859$ . There is also a secondary maximum of the central star formation at  $z = 0.799$  ( $\Delta C = 0.285$ ). At the maximum of star formation, this galaxy would be very bright ( $I_{814} = 17.74$ ) and it would be easily detectable in the HDF. Since no BCS as bright as this has

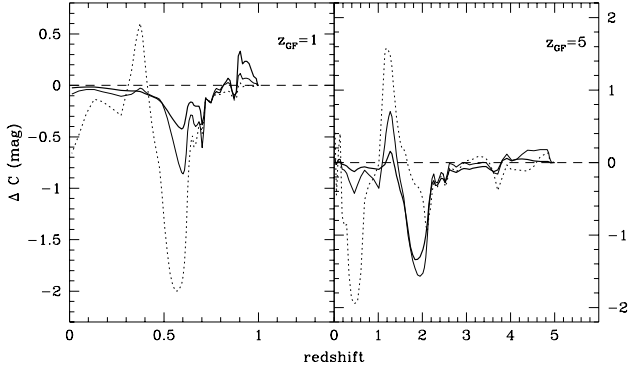


**Figure 3.** The same as Figure 2, but for the model with  $2 \times 10^{12} M_{\odot}$ . A  $\Omega_m = 0.3$ ,  $\Omega_{\Lambda} = 0.7$  cosmology is adopted here.

been detected in A99 sample, we can tentatively conclude that the typical BCSs are not  $\sim L^*$ -ellipticals formed at  $z_{GF} \sim 1$ . Turning to higher  $z_{GF}$ 's ( $z_{GF} = 5$ ), the blue core is more pronounced in the  $U_{300} - B_{450}$ , in which the maximum colour gradient occurs at  $z = 2.012$  ( $\Delta C = 1.851$ ). Note, however, that the model galaxy would be practically invisible in the  $U_{300}$  band ( $U_{300} = 29.51$  for the whole galaxy), while still detectable in other bands ( $B_{450} = 25.66$ ,  $V_{606} = 24.55$ , and  $I_{814} = 23.71$ ). As a matter of fact, it would be classified as a LBG, because its colours  $B_{450} - V_{606} = 1.11$  and  $U_{300} - B_{450} = 3.85$  satisfy the criteria for selecting LBGs at  $2 < z < 3.5$ :  $B_{450} - V_{606} \leq 1.2$  and  $U_{300} - B_{450} > B_{450} - V_{606} + 1.0$  (Dickinson 1998). Note that for a  $\Omega_m = 0.12$ ,  $\Omega_{\Lambda} = 0.88$  cosmology, the luminosity distance would be larger and the galaxy fainter:  $U_{300} = 31.05$ ,  $B_{450} = 27.97$ ,  $V_{606} = 26.23$ , and  $I_{814} = 24.99$  at  $z = 2$ . Then,  $B_{450} - V_{606} = 1.74$  and it would no longer be identified as a LBG.

### 3.2 A massive central galaxy in a cooling flow

Figure 3 shows the evolution of the colour gradient for the FT98 model with  $M_G = 2 \times 10^{12} M_{\odot}$ , which has a present-day stellar mass of  $2.4 \times 10^{12} M_{\odot}$ . Note that the late cooling flow episode in this model would require enough gas supply through the outer boundary of the galaxy, a condition that would be met if the galaxy would be located at the centre of a relaxed cluster of galaxies. As a matter of fact, the model with  $M_G = 2 \times 10^{12} M_{\odot}$  could represent an elliptical at the bottom of the potential well of a cluster of galaxies collecting the gas of a cooling flow formed in the intra-cluster medium, since the most massive central galaxies of cooling flows have masses of this order.

On the other hand, the early cooling flow episode could be maintained by the gas within the dark mass halo of the protogalaxy itself and thus would not require that the galaxy be located in a cluster, or, more properly speaking, that the protocluster containing the galaxy be well-developed.

In this model, the first episode of star formation is over a more extended region so the central colour gradient is smaller. In addition, for a galaxy formed at  $z_{GF} = 5$ , the reversal blue core/red core is followed by a contra-reversal red core/blue core due to later central star formation, which would correspond to the present-day central star formation

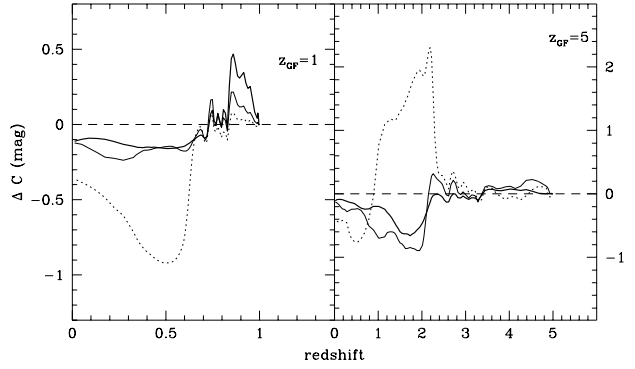


**Figure 4.** The same as Figure 3, but for the model with  $2 \times 10^{11} M_{\odot}$  and  $x_{SF} = 1/3$ .

activity seen in a few central dominant galaxies in cooling flows (McNamara 1997).

At late times, Model 20 shows starbursts in its core fed by the late cooling flow. As a consequence, as we approach  $z \sim 0$ ,  $\Delta C$  varies wildly, being positive most of the time (star formation in the core prevails).

### 3.3 Recurrent star formation in ellipticals

One particularly interesting model is the model 2(1/3) of FT98 because it exhibits recurrence of late central inflow episodes. This model has  $M_G = 2 \times 10^{11} M_{\odot}$ , as the fiducial model, but  $x_{SF} = 1/3$  instead of  $x_{SF} = 1/2$  —  $x_{SF}$  is the index of Schmidt law describing the dependence of the specific star formation rate on the gas density  $\nu_{SF} \propto \rho^{x_{SF}}$  (see end of Section 2). As the SN I rate decreases, the wind stalls, the gas starts to accumulate in the galaxy core, and the radiative losses drive a new central cooling flow. The late central inflow episodes are brief and quickly put out by the resulting burst of star formation. The duration of the late cooling flow episodes is a few times  $10^7$  yr, and, since the separation between them is typically a few Gyr, their duty cycle is  $\sim 1/100$ . The turning on and off of the central inflow could correspond to the “active” and “inactive” states of the core in both the super-massive black hole model of AGN and the starburst model of AGN. In addition, the length of the duty cycle of the central inflow increases with time and the amount of material deposited decreases, implying a steep decrease of the time-averaged luminosity of any central activity powered by the infalling material. For the model 2(1/3), the second central inflow occurs at  $t = 4$  Gyr and involves  $1.5 \times 10^7 M_{\odot}$ , and the third one ( $8.4 \times 10^6 M_{\odot}$ ) happens at  $t = 9.5$  Gyr. Each late central inflow episode is accompanied by enhanced star formation inside the central kpc, the signature of which is a temporary blueing of the galaxy core.

These late episodes of star formation of the model 2(1/3) imply that the blue core persists even at redshifts lower than in the fiducial model. This can be seen from the lower  $z_{rev}$  of the model 2(1/3) in comparison to that of model 2. For  $z_{GF} = 1$ , the first central cooling flow episode is more conspicuous in the  $V_{606} - I_{814}$ , as was the case for model 2. The maximum of the  $V_{606} - I_{814}$  colour gradient occurs at  $z = 0.853$  when  $\Delta C = 0.473$  (in the  $B_{450} - V_{606}$

colour,  $\Delta C = 0.222$ ). However, the second central cooling flow episode is more noticeable in  $B_{450} - V_{606}$ , corresponding to the local maximum  $\Delta C = 0.179$  at  $z = 0.744$  ( $\Delta C = 0.114$  in  $V_{606} - I_{814}$ ). The third inner cooling flow episode has a more pronounced signature in  $U_{300} - B_{450}$ , but the associated starburst is so weak that it does not change the redder core to a bluer core, so  $\Delta C = -0.012$  at  $z = 0.681$ . The metallicity gradient effect dominates over the impact of the star formation, as we can see from nearly constancy of the  $V_{606} - I_{814}$  colour gradient ( $\Delta C = -0.071$  at  $z = 0.681$ ).

### 3.4 Colour gradients as cosmological probes

Star formation activity in high redshifts galaxies has already been proposed to be used to determine the cosmological constant ( $\Omega_\Lambda$ ) and the matter mass density of the Universes ( $\Omega_m$ ) (Melnick, Terlevich & Terlevich 2000). We suggest here the use of colour gradients as a cosmological probe. The time-scales for the evolution of the central colour gradient in spheroids can potentially provide an independent clock for measuring the age of the Universe. Figures 2 also exhibits the results for three different cosmologies, illustrating the sensitivity of the evolution of the colour gradient to the value of  $\Omega_m$ . We consider a flat cosmology  $\Omega_m + \Omega_\Lambda = 1$  with  $0.12 \leq \Omega_m \leq 0.45$ , as favoured by the simultaneous constraints of the first acoustic peak of the angular power spectrum of the cosmic radiation background measured by the BOOMERang (de Bernardis et al. 2000) and the redshift-magnitude relation derived from high redshift supernovae surveys (Perlmutter et al. 1999, Riess et al. 1998, Schmidt et al. 1998). These latter works have already found evidence for an accelerating Universe in which matter would provide only  $\sim 30\%$  of the critical density for a flat Universe, with the rest being accounted for by the cosmological constant  $\Lambda$ . Therefore, the three cosmologies adopted here consider  $\Omega_m = 0.3, = 0.12$  and  $= 0.45$ .

An additional constraint is the age of the Universe given by each cosmology: 11.98, 13.47 and 17.09 Gyr, for  $\Omega_m = 0.45, = 0.3$  and  $= 0.12$ , respectively. The  $\approx 10\%$  errors on  $H_0$  prevent us from using values of  $H_0$  significantly lower than  $70 \text{ km s}^{-1} \text{ Mpc}^{-1}$ , so the age of the Universe implied by  $\Omega_m = 0.45$  would be dangerously low in comparison to the ages of the oldest globular clusters,  $\sim 11.5 - 14$  Gyr, derived in the post-HIPPARCOS age (D'Antona, Caloi and Mazzitelli, 1997; Salaris, degl'Innocenti and Weiss, 1997; Pont et al. 1998; Chaboyer et al. 1998; Carretta et al. 2000).

We should also take into account the constraints on the age of the Universe from high redshift old galaxies (Lima & Alcaniz 2000). One of the strongest lower limits on the age of the high redshift Universe comes from the very red galaxy 53W069 at  $z=1.49$ , with a minimal stellar age of 4.0 Gyr (Dunlop 1999), which, for  $H_0 > 60 \text{ km s}^{-1} \text{ Mpc}^{-1}$ , implies  $\Omega_m < 0.5$ .

A useful quantity that could be used to set the colour clock of the evolving spheroid and distinguish between several cosmologies and investigate the epoch of galaxy formation is  $z_{rev}$ . The cosmologies with smaller  $\Omega_m$ 's (larger  $\Omega_\Lambda$ 's) have larger lookback times, and therefore, higher  $z_{rev}$ 's.

Moreover, the models with masses around that of an  $L^*$ -elliptical progenitor ( $M_G = 10^{11} - 10^{12} M_\odot$ ) have  $z_{rev}$  remarkably similar, which guarantees a fair accuracy for the

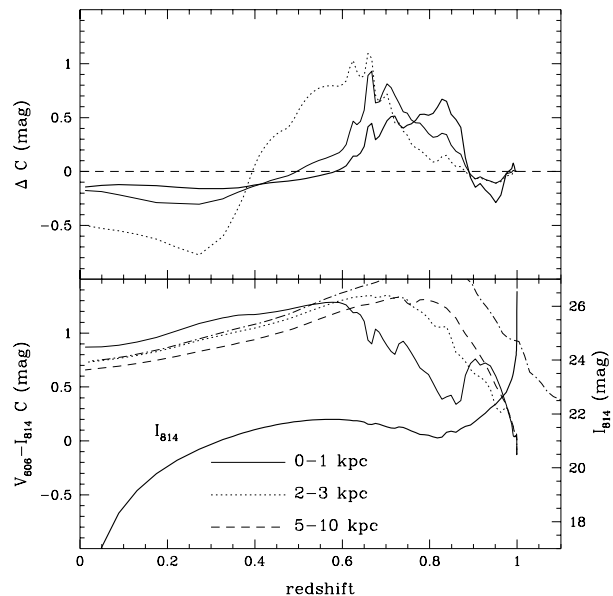


**Figure 5.** Top panel: evolution of the colour gradients  $\Delta C$  of the colours:  $V_{606} - I_{814}$  (heavy solid lines),  $B_{450} - V_{606}$  (light solid lines), and  $U_{300} - B_{450}$  (dotted lines), for the model with  $M_G = 5 \times 10^9 M_\odot$ , for the  $\Omega_m = 0.3, \Omega_\Lambda = 0.7$  cosmology and an epoch of galaxy formation  $z_{GF} = 1$ . Here  $\Delta C$  is defined as the colour seen inside the annulus  $2 < r < 3$  kpc minus the colour in the central kpc ( $r < 1$  kpc). Lower panel: evolution of the  $V_{606} - I_{814}$  colour through several annular apertures. The dot-dashed line represents the  $V_{606} - I_{814}$  colour through a  $2 < r < 3$  kpc aperture for  $z_{GF} = 1.2$ . Also given the evolution of  $I_{814}$  for the whole galaxy.

colour gradient clock. For a  $\Omega_m = 0.3, \Omega_\Lambda = 0.7$  cosmology, the model with  $10^{11} M_\odot$  has  $z_{rev} = 0.745$  ( $z_{GF} = 1$  and  $V_{606} - I_{814}$ ) and  $z_{rev} = 1.159$  ( $z_{GF} = 5$  and  $U_{300} - B_{450}$ ). The respective values for the model with  $10^{12} M_\odot$  are 0.806 and 0.970, and, for model 2, 0.764 and 1.263.

Model 20 is not particularly useful as a colour clock, due to the massive late cooling flow, which prevails at the present time. It is worth to note that if the model is old enough ( $z_{GF}$  high and  $\Omega_m$  low), there is central star formation driven by the late cooling flow. Therefore, as we can see from Table 1, the model galaxy has a bluer core at the present day for cosmologies and  $z_{GF}$ 's that imply larger lookback times till the epoch of galaxy formation,  $t_{b,GF}$ , and in this case  $z_{rev}$  is not defined.

### 3.5 Bluer Core Spheroids

It is interesting that the lower mass models of FT99, intended to describe typical LBGs with velocity dispersions around  $70 \text{ km s}^{-1}$  have properties that are similar to those of typical BCSs of A99 (for instance, BCS HDF-2.264 at  $z=0.478$ ). In particular, the models with  $M_G = 10^{10} M_\odot$  and  $5 \times 10^9 M_\odot$  have prolonged central star formation extending for more than 3 Gyr (see Figure 1 of FT99). Because of this, they could be seen as BCSs over a significant fraction of their lifetime. These objects, if they have been formed at

**Table 1.** The redshift of reversal from blue core to red core

$\Omega_m$	$z_{GF}$	Model 2			Model 2(1/3)			Model 20		
		$U - B$	$B - V$	$V - I$	$U - B$	$B - V$	$V - I$	$U - B$	$B - V$	$V - I$
0.12	1	0.835	0.805	0.809	0.780	0.777	0.779	0.388	0.852	0.851
0.30	1	0.792	0.759	0.764	0.729	0.725	0.730	0.311	0.814	0.814
0.45	1	0.763	0.729	0.735	0.695	0.693	0.698	0.268	0.789	0.791
0.12	2	1.640	1.746	1.589	0.927	1.444	1.536	...	...	...
0.30	2	1.517	1.463	1.450	1.176	1.272	1.382	0.624	0.691	1.575
0.45	2	1.447	1.366	1.370	1.089	1.190	1.296	0.528	0.598	1.506
0.12	3	1.093	2.367	2.372	0.882	1.958	2.023	...	...	...
0.30	3	1.690	2.325	2.001	0.913	2.305	1.898	...	...	...
0.45	3	1.886	2.227	1.865	1.378	2.198	1.755	0.678	0.758	2.452
0.12	5	0.853	2.823	3.540	0.772	2.416	2.789	...	...	...
0.30	5	1.263	2.864	3.438	0.899	2.153	2.713	...	...	...
0.45	5	1.457	2.752	3.240	0.868	1.959	2.059	...	...	...

$z_{GF} \sim 4 - 5$ , would be LBGs at  $z \sim 3$ , but if  $z_{GF} \sim 1$  instead, they would be classified as BCSs at  $z \sim 0.7$ .

Figure 5 illustrates the evolution of the colour gradients of the FT99 model with  $5 \times 10^9 M_\odot$  (hereafter model 0.05), assuming  $z_{GF} = 1$ . Model 0.05 would be seen as a  $\sigma = 55 \text{ km s}^{-1}$  LBG at an age of 0.5 Gyr, and as a present-day (age of 13 Gyr)  $0.05L^*$  spheroid. In this model, the central cooling flow is extinguished only at 3.63 Gyr. By comparison, in the fiducial model 2, the inner cooling flow ends at 1.80 Gyr. In order to compare our results with observations with the same resolution as those of HST as in A99, now  $\Delta C$  is defined as the colour inside the annulus  $2 < r < 3 \text{ kpc}$  minus the colour in the central kpc, since the WFPC-2 pixel size of  $0.1''$  corresponds to 0.6 kpc at  $z = 0.5$  for a  $\Omega_m = 0.3$ ,  $\Omega_\Lambda = 0.7$  cosmology. The resolution is even better in the colours  $V - I$  maps of A99, which have a drizzled pixel scale of  $0.04''$ , allowing, for instance, a clear definition of the  $r \approx 0.25''$  blue core of the BCS HDF-2.264. In addition, in this section, we use Vega magnitudes, as in A99.

As we see from Figure 5, for  $z > 0.6$ , our model galaxy would be easily detected as a BCS in the  $V_{606} - I_{814}$  colour, which is the more reliably determined colour in A99 (Menanteau et al. 2000). At  $z = 0.7$ ,  $\Delta C = 0.472$  and  $I_{814} = 21.52$ , while the colour gradient is flat in the outer part of the galaxy ( $V_{606} - I_{814}$  (2-3 kpc) = 1.354 and  $V_{606} - I_{814}$  (5-10 kpc) = 1.311). Note that the galaxy is detectable as a BCS at lower redshifts in  $B_{450} - V_{606}$  and  $U_{300} - B_{450}$  ( $z_{rev} = 0.583$ , 0.496 and 0.395 in  $V_{606} - I_{814}$ ,  $B_{450} - V_{606}$  and  $U_{300} - B_{450}$ , respectively). Model 0.05 was not tailored to reproduce the BCS HDF-2.264, but the similarities of the properties of the model to the object suggest that, if HDF-2.264 is typical of BCSs, they would be  $z \sim 0.5$  counterparts of sub- $L^*$  spheroids, since  $I_{814} = 21.73$  of the model at  $z = 0.5$  is comparable to  $I_{814} = 21.66$  (Menanteau et al. 2000) —  $I_{814}$  of our model varies within the range 21.2 – 21.8 between  $z = 0.4$  and  $z = 0.8$ .

The colours of the outer region (2–3 kpc) constrain the average age of the stellar population of the galaxy. Within the scenario of our model the colours of the outer parts of HDF-2.264 suggest  $z_{GF}$  somewhat higher than 1.0. As a matter of fact, model 0.05 has  $V_{606} - I_{814}$  (2-3 kpc) = 1.171 at  $z = 0.5$  for  $z_{GF} = 1$ , while it has  $V_{606} - I_{814}$  (2-3 kpc) = 1.223 at  $z = 0.5$  for  $z_{GF} = 1.2$ , thus reproducing well the red

outskirts of HDF-2.264, for which the reddest pixels have  $V_{606} - I_{814} \approx 1.3$ , with an error of 0.07 mag (see Figure 4 of A99).

On the other hand, the recent central star formation at  $z = 0.478$  of HDF-2.264 could be explained by some secondary central infall similar to that of model 2(1/3). Note that, at  $t = 1$  Gyr, the model 0.05 has a fully developed galactic wind with  $1200 \text{ km s}^{-1}$  at  $r = 10 \text{ kpc}$ . However, at  $t = 3$  Gyr, the galactic wind has weakened (wind velocity of  $270 \text{ km s}^{-1}$  at  $r = 10 \text{ kpc}$ ) and, in the inner regions there is only a highly subsonic outflow ( $20 \text{ km s}^{-1}$  at  $r = 1 \text{ kpc}$ ). The gas accumulated in the dark halo of the galaxy brakes the outflowing gas, so it is possible that, in some cases, the core accumulates enough gas returned by the evolving stars to trigger late central star formation episodes. (this happens in model 2(1/3) but for a  $\sim L^*$  galaxy). In this connection, we could explain the scarcity of BCSs in galaxy cluster environments (Menanteau et al. 2000) as due to the stripping of the gas in the dark halo of the spheroid, thus preventing very prolonged ( $> 3$  Gyr) cooling flow-fed central star formation as well as late recurrent central star formation episodes.

## 4 CONCLUSIONS

The early-type galaxies with blue cores of A99 are very symmetrical, showing no morphological peculiarity. A99 points out that the  $\sim 40\%$  fraction they find for the early-type systems with recent star formation is consistent with the predictions from hierarchical models. However, in the hierarchical model scenario, after a merger event, the resulting system has to relax quickly enough in order to be classified as an early-type galaxy.

An alternative scenario to the merger picture would be that proposed by the multi-zone single-collapse model, in which late gas central inflow would feed star formation in the core of the galaxy. A spherically symmetrical star forming population would naturally develop in the centre of the galaxy, and one would not need the extra ingredient of a short relaxing time-scale as in the merger scenario.

The central blue cores arise naturally in our models, in this way reproducing the colour gradients which are typical of BCSs. Within the scenario of our model, if the HDF-2.264 BCS at  $z = 0.478$  is typical of BCSs, then they are  $z \sim 0.5$

counterparts of sub- $L^*$  spheroids, formed at redshifts somewhat larger than  $z_{GF} = 1$ , and requiring very prolonged ( $> 3$  Gyr) cooling flow-fed central star formation or recurrent central star formation episodes. This could account for the scarcity of BCSs in rich clusters due to the removal of the gas in the dark halo of the spheroid by the intracluster medium. Without the gas reservoir in the dark halo, the gas inside the galaxy would escape very rapidly, thus preventing any long term cooling flow that could feed very prolonged central star formation activity. At the same time, any late central starburst would be suppressed, since it could not be fed either by gas ejected by evolved stars and accumulated in the galaxy or by old galactic wind ejecta braked in the gas-filled dark matter halo and falling back towards the galaxy.

If the progenitors of  $\sim L^*$  spheroids were formed at redshifts larger than  $z_{GF} = 1$ , they would give rise to high-mass, high-redshift counterparts of the  $0.4 < z < 1$  BCSs. If they are formed at  $z_{GF} \sim 5$ , they could be missed in the standard multi-colour surveys designed to select candidates to LBGs. Although it is possible to find some BCSs in the present LBG samples, the colour criteria used in searching LBGs should be made more flexible (for instance, redder  $B_{450} - V_{606}$  colour indices) in order to search for high-redshift BCSs which would be the  $\sim 0.3$ -a few Gyr old progenitors of the present day  $\sim L^*$  ellipticals. Moreover, according to the chemodynamical model for evolution of spheroids, due to the fact that the prolonged central star formation characteristic of BCSs, extends at least 2 Gyr, and, sometimes, longer than 3 Gyr, the BCS stage in the evolution of spheroids lasts somewhat longer than the LBG stage ( $0.2 \lesssim t \lesssim 1.5$  Gyr) (FT99) and should also be found in abundant numbers at high redshifts, provided that we explore regions in the colour diagrams wider than those used in the selection of LBG candidates, and perform deeper imaging with higher resolution of the candidates to BCSs. Finally, these high-redshift BCSs would be useful probes for the epoch of galaxy formation and the cosmological parameters of the Universe.

## ACKNOWLEDGMENTS

We thank Gustavo Bruzual for making us available the GISSEL code for evolutionary stellar population synthesis. We are grateful to the referee for a number of suggestions that made this paper more readable. A.C.S.F. acknowledges support from the Brazilian agencies FAPESP, CNPq, and FINEP/PRONEX.

## REFERENCES

- Abraham R.G., Ellis R.S., Fabian A.C., Tanvir N.R., Glazebrook K., 1999, MNRAS, 303, 641
- Barger, A.J., Cowie, L.L., Trenham, N., Fulton, E., Hu, E.M., Songaila, A., Hall, D., 1999, AJ, 117, 102
- Chaboyer B., Demarque P., Kernan P.J., Krauss L.M., 1998, ApJ 494, 96
- Carretta E., Gratton R.G., Clementini G., Fusi Pecci F., 2000, ApJ, 533, 215
- D'Antona F., Caloi V., Mazzitelli I., 1997, ApJ 477, 519
- de Bernardis P., et al., 2000, Nature, 404, 955
- Dickinson M., 1998 in Livio M., Fall S.M., Madau P., eds, The Hubble Deep Field. C.U.P., Cambridge, p. 219.
- Dunlop J.S., in Rottgering H.J.A., Best P., Lehnart M.D., eds, The Most Distant Radiogalaxies. Kluwer, Dordrecht, p. 71
- Friaza A.C.S., Terlevich R.J., 1998, MNRAS, 298, 399
- Friaza A.C.S., Terlevich R.J., 1999, MNRAS, 305, 90
- Friaza A.C.S., Viegas S.M., Gruenwald R., 1998, in P. Petitjean, S. Charlot, eds, Structure and Evolution of the Intergalactic Medium from QSO Absorption Line Systems. Editions Frontières, Paris, p. 406
- Grevesse N., Anders E., 1989, in Waddington C.J., ed., Cosmic Abundances of Matter. AIP, New York, p.183
- Guhathakurta P., Tyson J.A., Majewski S.R., 1990, ApJ, 357, L9.
- Hamann. F., Ferland G., 1993, ApJ, 418, 11
- Jimenez R., Friaza A.C.S., Dunlop J.S., Terlevich R., Peacock J.A., Nolan L.A., 1999, MNRAS, 305, L16
- Lima J.S., Alcaniz, J.A.S., 2000, MNRAS, 317, 893
- McNamara B.R., 1997, in Soker N., ed., ASP Conf. Ser. 115, Galactic and Cluster Cooling Flows. Astron. Soc. Pac., San Francisco, p. 147
- Melnick J., Terlevich R., Moles M. 1988, MNRAS, 235, 297
- Melnick J., Terlevich R., Terlevich E., 2000, MNRAS, 311, 629
- Menanteau F., Abraham R.G., Ellis R.S., 2000, astro-ph/0007114
- Mould J.R., et al. 2000, ApJ, 529, 726
- Perlmutter S., et al., 1999, ApJ, 517, 565
- Pont F., Mayor M., Turon C., Vandenberg D.A., 1998, A&A, 329, 87
- Riess A.G., Filippenko A.V., Challis P., et al., 1998, AJ, 116, 1009
- Salaris M., degl'Innocenti S., Weiss A., 1997, ApJ, 479, 665
- Schmidt B.P., Suntzeff N. B., Phillips M. M., et al., 1998, ApJ, 507, 46
- Steidel C.C., Pettini M., Hamilton D. 1995, AJ, 110, 2519
- Steidel C.C., Giavalisco M., Pettini M., Dickinson M., Adelberger K.L., 1996, ApJ, 462, L17
- Zepf, S.E., 1997, Nat, 390, 377.

This paper has been produced using the Royal Astronomical Society/Blackwell Science L<sup>A</sup>T<sub>E</sub>X style file.